Journal of Chromatography A, 1218 (2011) 3095–3104

Contents lists available at ScienceDirect

Journal of Chromatography A

journal homepage: www.elsevier.com/locate/chroma

Understanding mechanisms of pressure-assisted electrokinetic injection: Application to analysis of bromate, arsenic and selenium species in drinking water by capillary electrophoresis-mass spectrometry

Huijuan Zhang[1], Jennilee Gavina, Yong-Lai Feng*

Exposure and Biomonitoring Division, Health Canada, AL: 0800C, EHC, Tunney's Pasture, Ottawa, Ontario K1A 0K9, Canada

ARTICLE INFO

Article history:
Received 29 December 2010
Received in revised form 1 March 2011
Accepted 9 March 2011
Available online 17 March 2011

Keywords:
Pressure-assisted electrokinetic injection
Inorganic anions
Water contaminants
Capillary
eletrophoresis-electrospray-tandem mass spectrometry
Sample pre-concentration
Band broadening

ABSTRACT

The mechanism underlying the enrichment power by pressure-assisted electrokinetic injection (PAEKI) in capillary electrophoresis (CE) was investigated for on-line pre-concentration of arsenic [As(III) and As(V)], selenium [Se(IV) and Se(VI)] and bromate (BrO_3^-). Analyte diffusion behaviour from PAEKI sample plugs were evaluated by monitoring peak broadening as a function of stagnant time and position in the capillary. During PAEKI, anionic analytes accumulate at the sample-separation buffer boundary. We proposed that a counter-ion layer formed in PAEKI, where a cation layer was formed at the separation buffer side of boundary. The cation layer served as a soft boundary which impeded zone broadening via electrostatic attraction between layers. This effect likely played an important role in maintaining focused analyte bands by suppressing diffusion. Comparison of analyte behaviour in PAEKI injected sample plugs to behaviour in hydrodynamically injected ones proved the existence of a counter-ion layer. The dependence of analyte diffusion in PAEKI plugs on electrochemical properties (viscosity, conductivity, electrophoretic mobility) further supported the hypothesis. Additionally, it was noted that analytes with low electrophoretic mobility were more efficiently pre-concentrated by PAEKI and were less subject to forces of dispersion than analytes with greater electrophoretic mobility. PAEKI-CE coupled to electrospray tandem mass spectroscopy (ESI-MS/MS) was then optimized and validated for detection of arsenic, selenium and bromate in water samples. On-line enrichment of the target analytes was achieved with 1–3 ng mL^{-1} detection limits, which was below the maximum contaminant levels in drinking water for all five anions studied. Noteworthy, the potential of the method for unbiased detection of molecular species in untreated water was demonstrated. No contamination was detected in the water samples tested; however, recovery was 90–118% for spiked samples. The method was demonstrated be comparable to current methods for detection of inorganic contaminants in drinking water and is a good alternative method to ion chromatography/liquid chromatography–MS.

1. Introduction

In order to protect public water systems, drinking water is often processed prior to public distribution by chlorination or ozonation. However, these disinfection processes can be insufficient for removal of trace metals and may further produce by-products hazardous to human health [1–3]. Inorganic anions, such as bromine, arsenic and selenium species are routinely monitored in drinking water due to their negative health effects [4,5]. Bromate (BrO_3^-), a major inorganic disinfection by-product in drinking water from ozonation of surface waters containing bromide, is considered as a genotoxic carcinogen [6,7]. A maximum contaminant level (MCL) of 10 ng mL^{-1} has been imposed in drinking water by EPA [8]. Of trace metal contamination, the most notable incidence of arsenic in groundwater; however, contamination occurred in Bangladesh in the mid-1990s [4]. In this occurrence, arsenic was leached from natural deposits into the groundwater however contamination can also result from runoff of industrial origins such as mining, smelting and paper production [9]. Poisoning has been shown to be linked to cancer but also can cause neurological effects, hypertension and cardiovascular disease, pulmonary disease, diabetes mellitus, and circulatory problems [10]. In general, the toxicity depends both on oxidation state and whether As is present in an organic or organic form [11]. Selenium, another naturally occurring metal, is essential for human health, but is also toxic at high doses and is therefore regulated by the EPA. A selenium deficiency can lead to necrotic degeneration of liver, pancreas, heart and kidney and sometimes can increase the risk of cancer [12]. However,

* Corresponding author. Tel.: +1 613 948 5804; fax: +1 613 946 3573.
E-mail address: yong-lai.feng@hc-sc.gc.ca (Y.-L. Feng).
[1] Current address: College of Chemistry and Materials, South-Central University of Nationalities, 430074 Wuhan, China.

0021-9673/$ – see front matter.
doi:10.1016/j.chroma.2011.03.017

toxic doses lead to selenosis which can cause serious damage to the nervous system [13]. The MCL has been set to 10 ng mL^{-1} for total arsenic and 50 ng mL^{-1} for total selenium in drinking water to protect consumers served by public water systems from the effects of long-term, chronic exposure to these chemicals. Detection methods must therefore be highly sensitive in order to detect arsenic and selenium in drinking water. Methods for routine measuring trace inorganic anions in drinking water currently include ion chromatography (IC) and high performance liquid chromatography (HPLC) [14,15]. However, MCL does not differentiate between inorganic, organic species or species oxidation states. This information would be useful in drinking water analysis as arsenic and selenium species with oxidation states give different toxicities and species type also provides useful information for water treatment strategy.

Capillary electrophoresis (CE) is a powerful separation technique capable of rapid, high resolution separation of a wide range of charged and neutral analytes from a variety of sample matrices [16,17]. It therefore represents a promising alternative method for measurement of inorganic contaminants in water. There are many reports of inorganic ion analysis by CE [18,19], however CE still lags behind HPLC for routine water analysis. This is due in part to the very small injection volume (nL) of CE compared to conventional injection (μL) in IC and HPLC, which limits the amount of sample that can be loaded onto the column and has greatly compromised application of CE for trace analysis of dilute samples. In order to increase the sample injection amount, several enhancement techniques have been developed including transient on-column isotachophoresis (ITP), sample stacking, sweeping, dynamic pH junction, and countercurrent electroconcentration, the latter including electrocapture and head column field-amplified sample stacking (HC-FASS) [20,21]. In most of the above techniques, the mechanism of pre-concentration occurs in-column and results in focusing of a large sample band during electromigration. Focusing is made possible by differences in the ionic strength (stacking), chemical composition (sweeping) or pH between the sample plug and background electrolyte (BGE). These focusing techniques allow large plugs of sample to be loaded onto the capillary column (>1% capillary volume) with typical enhancement factors in a range of 10^1–10^3. The mechanism of focusing occurs in-column, thus these methods are amenable to automation on commercial instruments. They are, however, limited by the dimensions of the capillary which defines the maximum amount of sample that can be loaded. In order to overcome this drawback, sample pre-concentration methods which utilize the bulk sample solution have also been developed.

Countercurrent electroconcentration techniques utilize a counterflow to capture charged analytes from the bulk sample solution during electromigration. Analytes are typically concentrated in an electric field by balancing the electrophoretic velocity with a hydrodynamic counterflow [22,23]. In HC-FASS, forces are balanced at the capillary inlet, which increases the concentration of analyte at the head of the column allowing very dilute solutions to be used for injection. Kaljurand and coworkers were able to sample from solutions as dilute as 5 ppb [24]. Swerdlow and coworkers applied similar principles to a microfluidic platform where analytes were concentrated at a specific position within the capillary, thereby avoiding potential sample loss [25]. The group of M. Lee further contributed to the approach by utilizing a dialysis fibre as the separation capillary which allowed an electric field gradient to be created across the capillary. The counterflow was set as to focus multiple protein analytes in the column where their electrophoretic velocities balanced with the counterflow [26]. They further demonstrated in a subsequent report that electroosmotic flow could also be used as the counterflow force and that focusing was stable even at an exacerbated sampling time of 200 min [27]. Along with these initial reports, there have been several improvements and applications by Astorga-Wells et al. for the preconcentration of biomolecules with coupling to sample clean-up and further processing [28–30]. Countercurrent electroconcentration therefore offers the potential advantage of incorporating multiple sample preparative steps with high enhancement factors of (up to 15 000-fold enhancement) [31]. However, there are also several disadvantages since many of the above reports utilize homemade devices that operate external to the separation capillary.

In order to improve upon existing pre-concentration methods while overcoming the limitations of capillary dimensions, techniques which utilize multiple mechanisms have been developed. Electrokinetic injection with sweeping has been utilized by Quirino and Terabe in order to accomplish one million-fold enhancement [32] while Breadmore reported unlimited volume stacking by combining stacking with ITP in a method referred to as electrokinetic supercharging [33,34]. Routine use of these methods, however, are not straightforward as optimization is required for both steps; the electrokinetic injection and sweeping steps in the former and the ITP and stacking steps in the latter. We have developed the pressure assisted electrokinetic injection (PAEKI) method of sample pre-concentration, which utilizes principles of both countercurrent electroconcentration and stacking. In PAEKI, the sample consists of ionized analytes at an ionic strength much lower than that of the BGE. During injection the velocity of electroosmotic flow (EOF) is balanced to an external hydrodynamic pressure as to create a stationary boundary at the inlet of the capillary where the target analytes accumulate according to stacking principles. Like the above methods, this approach allows potential unlimited volume pre-concentration, however application of the method is simplified since no leading electrolyte is required and the stacking requirement for the sample can be met by simple dilution. This method has been successfully applied for concentrating single nucleotides, oligonucleotides, monophthalates and halogenated phenols [35–38]. Like previous countercurrent electroconcentration techniques, PAEKI can provide powerful enhancement factors where enhancement is dependant only on sampling time. Additionally, PAEKI is compatible with commercially available CE instrumentation, is not limited by the capillary dimensions and allows pre-concentration without compromising the separation efficiency, unlike with sample stacking and sweeping.

Although the powerful pre-concentration ability of PAEKI has been previously demonstrated, the working mechanism of how the sample plugs injected by PAEKI remained focused despite the long injection time has not been well-studied. Those mechanisms in the pre-concentration techniques aforementioned are not directly applicable to interpret it either. It was previously hypothesized that a soft boundary which formed at the interface of the sample and BGE zones was likely responsible for the narrow sample plug size in PAEKI [37]. To improve our understanding of the mechanisms underlying focusing in PAEKI, the current study is aimed at elucidating the nature of the sample zone injected. Peak width at full-width at half maximum (FWHM) of analyte peaks was employed as the indicator of interaction among ions in sample plugs introduced by either PAEKI or hydrodynamic injection at the BGE boundary. The nature of diffusion in a stagnant sample zone, by PAEKI or hydrodynamic injection, was investigated to determine the influences on focusing in the PAEKI process as well as to probe for the formation of possible counter-ion layers at the sample-BGE boundary. We further extended the application of PAEKI to analysis of inorganic disinfection by-products in drinking water by CE-MS/MS without any sample pre-treatment. Significantly, we were able to avoid the biases to speciation that can result from sample pre-treatment which allowed us to quantitate bromate, arsenite, arsenate, selenite and selenate in water samples with ng mL^{-1} detection limits.

2. Materials and methods

2.1. Reagents

2′-Deoxyadenosine-5′-monophosphate sodium salt (d-AMP, 98+%), sodium arsenate dibasic heptahydrate ($Na_2HAsO_4{\cdot}7H_2O$ (As(V)), 98+%, ACS reagent), sodium (meta)arsenite ($NaAsO_2$ (As(III)), ≥99%), sodium selenite (Na_2SeO_3 (Se(IV)), 99%), sodium selenate decahydrate ($Na_2SeO_4{\cdot}10H_2O$ (Se(VI)), 99%) and sodium bromate ($NaBrO_3$, 99+%), and ammonium carbonate (ACS reagent) were purchased from Sigma-Aldrich (Oakville, Ontario, Canada). Acetonitrile (ACN; high purity solvent, OmniSolvent) was obtained from EMD Chemicals (Gibbstown, NJ, USA) Sodium hydroxide solutions (0.1 and 1 mol L^{-1}) were purchased from Agilent Technologies Inc. (Waldbronn, Germany). De-ionized (DI) water was made in house by a Milli-Q system (Millipore, Bedford, MA).

2.2. Preparation of solutions

The stock solutions of 10 mg mL^{-1} of d-AMP, As(V), As(III), Se(IV), Se(VI) and BrO_3^- were prepared in DI water. The d-AMP solution was stored at −20 °C and the latter four solutions were stored at 4 °C until use. A 200 mmol L^{-1} stock solution of ammonium carbonate was made by dissolving 3.903 g of ammonium carbonate in 250 mL of DI water followed by adjustment of pH to 9.2 with 20% ammonium hydroxide. The buffer stock solution was stored at 4 °C. Working buffer solutions of ammonium carbonate were made from diluting the stock solution to the required concentrations with DI water and re-adjusting the pH to 9.2 with 10% ammonium hydroxide solution. All working buffer solutions were filtered by 0.2 μm syringe filters (Fisher Scientific, Ottawa, CA) and further degassed for 5 min by a sonication (Fisher Scientific, Ottawa, CA) before use.

2.3. CZE/UV conditions for study of plug behaviour

An Agilent Capillary Electrophoresis (3D-CE system) with a built-in Diode-Array Detector (DAD; Agilent Technologies Inc., Waldbronn, Germany) was used. Agilent CE ChemStation was used for the instrument control, data acquisition, and data analysis. The CE capillary column was 75 cm total length (L_T) of bare fused-silica column (66.5 cm of effective length to detector, L_d) with 50 μm inner diameter (i.d.; Polymicro Tech. LLC, Phoenix, AZ, USA). The new capillary was conditioned by flushing the column with 1 mol L^{-1} of sodium hydroxide solution for 10 min, DI water for 10 min and the running buffer (background electrolyte, BGE) for 10 min, in that order. The column cassette temperature was set at 20 °C. The DAD wavelength was set at 260 nm for d-AMP, and 195 nm for As(III), Se(IV) and BrO_3^-, respectively.

For comparative studies between PAEKI and hydrodynamic injections, experimental conditions were as follows. For hydrodynamic injection, 500 μg mL^{-1} of d-AMP was injected for 5 s with +50 mbar of hydrodynamic pressure resulting in a sample zone volume of 0.57 nL (0.29 ng d-AMP). After the injection, +30 kV was applied across the capillary for 0.5, 4.0, or 7.5 min to migrate of the injected sample zone to a position in the column of 5, 50, or 95% of the L_d ($v_{d\text{-}AMP}$ = 8.42 cm min^{-1}). The voltage was then removed and the sample plug was allowed to diffuse in 0 V cm^{-1} electric field for a certain stagnant time. In PAEKI injection, a sample containing 500 ng mL^{-1} of d-AMP was injected by application of simultaneous positive pressure of 50 mbar and negative voltage of 6 kV to the inlet end of capillary for 3 min, unless otherwise noted. Similarly to hydrodynamic injection, the injected sample plug was migrated to 5, 50 or 95% of the L_d and FWHM was calculated as a function of stagnant time. By peak area and peak height, the injected amount of d-AMP in PAEKI was similar to the amount injected by hydrodynamic injection. All separations were then conducted at +30 kV. The peak area, peak height and FWHM were integrated and calculated with the Agilent ChemStation software, respectively.

For studies determining the influence of analyte type, PAEKI injections were performed under pressure and voltage conditions above, however the sample solution was a mixture of d-AMP, AsO_4^{3-}, SeO_3^{2-} and BrO_3^-. Sample concentrations and PAEKI duration, given in Table 1, were adjusted to ensure the final amount of analyte injected was constant. Separations were conducted at +30 kV immediately following PAEKI injection.

2.4. PAEKI-CE-ESI-MS/MS analysis of drinking water

Tap water samples from two office buildings and two residential houses were collected following the EPA method [39]. Briefly, 40-mL water was collected in clean amber glass bottles and stored at 4 °C before use. For each sampling site, a 40-mL sampling vial filled with DI water was used with the transportation and the sampling process as the field bank. Since drinking water samples presumably have a simple matrix, they were suitable for use by PAEKI without the need for any further pre-treatment. The samples were analyzed by the addition method. Addition was accomplished by spiking 1 mL samples with 10 μL of DI water for the controls and 5 or 50 mg L^{-1} of spiking solution prepared in DI water. Spiking solutions contained a mixture of the five analyte standards under study. The final analyte concentration levels after addition were 50 and 500 ng mL^{-1}. Calibration curves were constructed for As(III), As(V), Se(IV), Se(VI) and BrO_3^- from 5 to 5000 ng mL^{-1}, using 500 ng mL^{-1} d-AMP as the internal standard. Calibration standards were analyzed using PAEKI-CE-MS/MS via peak area. The calibration curves were subsequently obtained by plotting the ratios of peak areas of target analytes and the internal standard against the ratios of the corresponding concentrations. The five regression lines had R^2 coefficients all over 0.99.

All samples were analyzed by PAEKI-CE-MS/MS on an Agilent 3D-CE instrument linked to a 4000 QTRAP mass spectrometer (Applied Biosystems, Canada). The Agilent CE instrument controlled by the ChemStation software was used to inject samples via PAEKI and separate analytes injected. The 4000 QTRAP was controlled by the Analyst software and was used for monitoring the analytes with multiple reaction monitoring (MRM) in negative ion mode. The flow rates were 20 L min^{-1} of nitrogen for the curtain gas (CUR), 2 L min^{-1} of nitrogen for the collision gas (CAD) and 5 L min^{-1} of zero air for the ion source gas. The ion spray voltage (IS), the entrance potential, and the collision exit potential were set to −5300, −10 and −5 V, respectively. Other MS parameters are outlined in Table 2. The sheath liquid was prepared by adding 10% (v/v) DI water to a solution of isopropanol and methanol, 2:1 (v/v), for a final volume concentration of 60% isopropanol, 30% methanol and 10% water. The sheath liquid flow rate was set to 3 μL min^{-1}. A new capillary (L_T = 110 cm; i.d. = 50 μm) was conditioned and used in this system. The capillary temperature was room temperature. All samples were injected by simultaneous application of −7.5 kV and +50 mbar external pressure to the sample vial at the capillary inlet for 3 min. After injection, +30 kV plus +50 mbar of external pressure were applied for separation.

3. Results and discussion

It has been noted in our previous work that PAEKI offers a narrow, concentrated sample zone despite long injection times [35–37]. In this study, we continue to investigate the nature of PAEKI injection zones using d-AMP to probe mobility at the sample zone and BGE boundary. We further apply our findings to analyze the behaviour of inorganic anions and demonstrate the feasibility of

Table 1
The concentrations of analyte ions and corresponding PAEKI times.

Analyte	PAEKI duration (min) and corresponding analyte concentration (ng mL^{-1})					
	0.5	1	1.5	2	3	4
d-AMP	500.0	250.0	166.7	125.0	83.3	62.5
AsO_4^{3-}	250.0	125.0	83.3	62.5	41.7	31.3
SeO_3^{2-}	100.0	50.0	33.3	25.0	16.7	12.5
BrO_3^-	200.0	100.0	66.7	50.0	33.3	25.0

Capillary column: 75 cm of total length with i.d. 50 μm, 66.5 cm of effective length. *Buffer condition*: 20 mmol L^{-1} of ammonium carbonate with pH 9.2. *PAEKI conditions*: various injection times listed in the table with −6 kV plus 50 mbar, all samples were diluted in DI water.

PAEKI with CE-MS to monitor disinfection by-products in drinking water.

3.1. Counter-ion layer theory

In hydrodynamic injection, the initial distribution of analytes in a sample plug within the capillary should be identical to that of the solution in the sample vial. This is different from PAEKI where sample concentration occurs during injection based on stacking principles. An illustration of PAEKI for injection of anionic analytes is given in Fig. 1a. The capillary is initially filled with separation buffer before the sample vial is positioned at the capillary inlet. The conductivity of the sample solution is significantly lower than that of the BGE. Stacking therefore occurs at the boundary layer due to differences in conductivity; however injection is accomplished electrokinetically where the electric field bias aids in concentration of anions into the capillary. Since injection is under negative polarity, a positive external pressure is simultaneously applied in PAEKI in order to balance the opposite EOF to achieve a stationary boundary and meanwhile prevent migration of the analyte out of the capillary. Under these conditions, the amount of sample injected depends on the following equation:

$$N_i(t) = \gamma \mu_{ep,A} E_{inj} A C_{inj} t \quad (1)$$

where γ is the ratio of resistivity (ρ) of the sample medium and the BGE, $\mu_{ep,A}$ the electrophoretic mobility of the analyte in the sample solution, A the cross-sectional area of the capillary, E_{inj} is the electric field (generated by the injection voltage, V_{inj}), C_{inj} the concentration of analyte in the sample solution and t the injection time. Separation is then accomplished under normal positive polarity without external pressure, where samples containing mixtures of charged analytes can then resolved based on differences in $\mu_{ep,A}$.

During PAEKI injection, while anionic analytes concentrate at the stationary boundary forming an anion layer via stacking, the increase in negative charge at this interface (Fig. 1a) would generate the formation of a cation layer at the BGE side of the boundary due to electrostatic attraction. When the plug is subsequently migrated a short time (such as 0.5 min) by switching the applied voltage from negative to positive, the counter-ion layers would be held together by electrostatic attraction and remain intact (Fig. 1b).

Given that the major contribution to band-broadening is longitudinal diffusion, the formation of the soft counter-ion layer would have several implications to band broadening of the sample plug. In the absence of external forces, band broadening in CE is predominantly reflective of the diffusion behaviour of the analytes. During PAEKI, the formation of a cation layer at the boundary would decelerate stacked analyte anions migrating through due to the attractive interaction between the counter-ions, resulting in the observed narrow sample zone by decreasing extent of lateral diffusion. Most importantly, the electrostatic attraction between the counter-ion layers impedes the lateral diffusion of analytes in 0 V cm^{-1}, giving a different diffusion profile comparing to in a homogenous sample zone such as injected by hydrodynamic injection. When the plug is migrated for 4.5 min to a position of 50% L_d, the ion layers would become physically separated to a certain degree within the capillary due to $\mu_{ep,A}$ differences (Fig. 1c). As electromigration continues, for instance, 7.5 min to 95% L_d, the counter-ion layer becomes fully damaged and forces of diffusion may not be disrupted by the attractive interaction (Fig. 1d), thereby yielding band broadening profiles in 0 V cm^{-1} similar to hydrodynamically injected sample plug in which no kind of counter-ion layer exists to suppress diffusion. We therefore have compared band broadening between sample plugs injected by PAEKI and hydrodynamic injection as a function of time and position in the capillary. Like the electrical double layer which forms at the capillary wall during CE, the stability of the counter-ion layer would be affected by the relative viscosity (η) and permittivity of the BGE (ϵ), as well as the electrophoretic properties of the analyte including η, charge (z) and hydrodynamic size (R_H), which is inversely related to the diffusion coefficient (D).

3.2. Effect of diffusion time and position

As aforementioned, in the absence of any external forces (i.e. electric field or hydrodynamic pressure), band broadening represents the diffusion behaviour of the analytes in the sample plug. In an electropherogram, the broadening of a resulting peak can be measured as the peak width at half the maximum peak height, i.e. full-width at half maximum (FWHM). The diffusion profiles of sample plugs injected by PAEKI or hydrodynamically were compared as a function of diffusion time and position within the capillary in order to determine whether a counter-ion layer was indeed formed in PAEKI injections and if so, what forces would affect stabilization of such layer.

First, it was noted that the relationship between peak width and stagnant time was linear for sample injected hydrodynami-

Table 2
MRM parameters.

Analyte	Precursor species	Precursor (m/z)	Product species	Product (m/z)	Collision energy (V)
Arsenic	$As(III)O_2^-$	107	$As(III)O_2^-$	107	−30
	$H_2As(V)O_4^-$	141	$As(V)O_2^-$	107	−50
Selenium	$H^{80}Se(IV)O_3^-$	129	$^{80}Se(IV)O_2^-$	112	−50
	$H^{80}Se(VI)O_4^-$	145	$^{80}Se(VI)O_3^-$	128	−50
Bromate	$^{79}BrO_3^-$	127	$^{79}BrO^-$	95	−50
d-AMP	$C_{10}H_{13}N_5O_6P$	330	$C_5H_4N_5^-$	134	−30

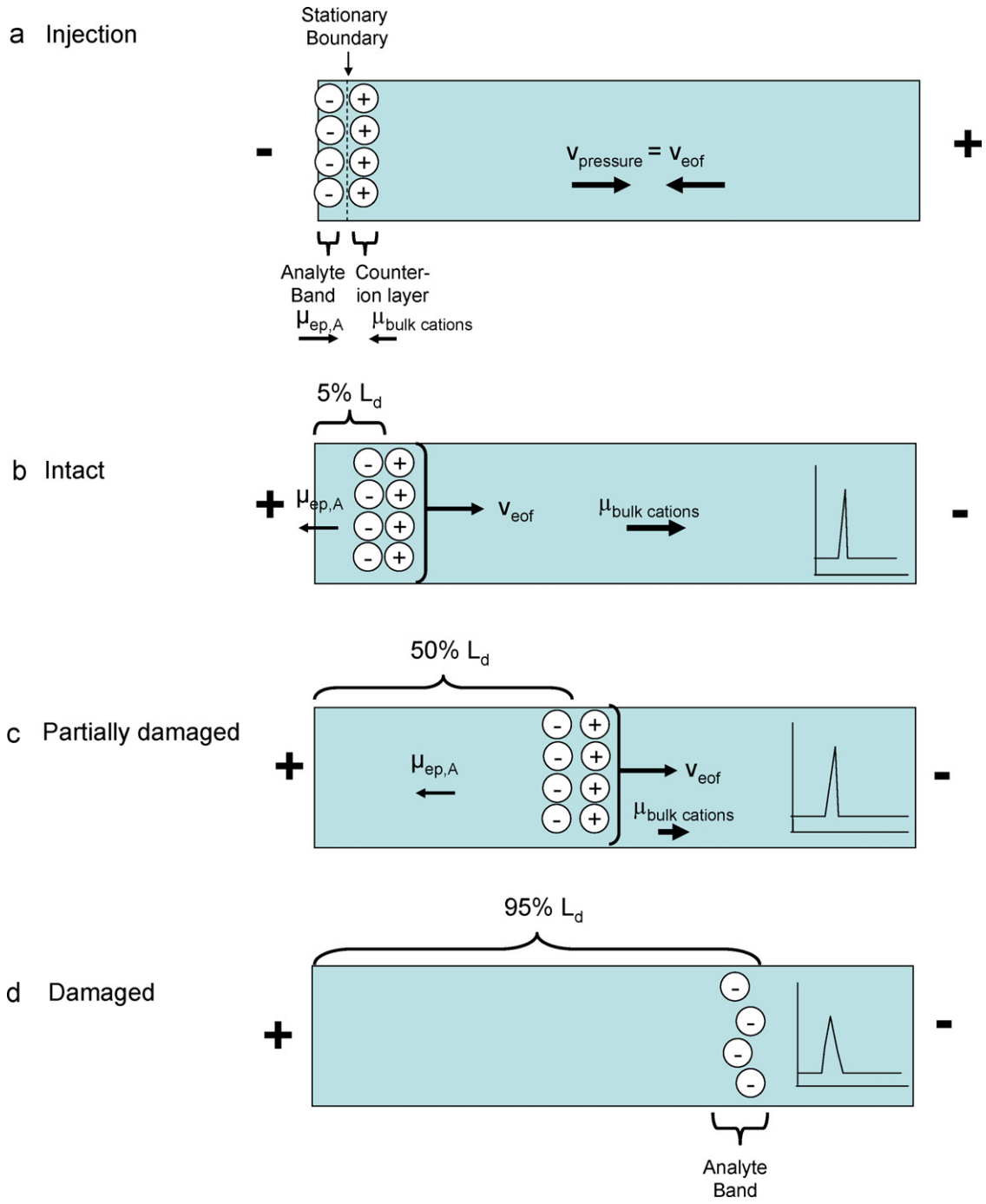

Fig. 1. Depiction of the behaviour of a theoretical counter-ion layer formed in PAEKI-CE. (A) Injection of negative analytes by PAEKI by application of a negative electric potential across the capillary (reverse polarity) and simultaneous external pressure to balance the magnitude of the electroosmotic flow. A counter-ion layer forms due to electrostatic attraction to the analytes accumulating at the stationary boundary. (B) Intact counter-ion layer during a short time of migration. (C) Partial disruption of the counter-ion layer by continued electromigration. (D) Full disruption of the counter-ion layer during a long time of electromigration.

cally, regardless of the position in the capillary where the sample zone was allowed to diffuse (Fig. 2). On the contrary, PAEKI sample zones exhibited a non-linear relationship as a function of stagnant time. Interestingly it was observed that peak broadening initially did not occur for PAEKI injected analytes at 5 and 50% L_d positions for the first 30 min. After 30 min, which will be referred to here as the "threshold" time, broadening occurred in non-linear fashion initially and occurred in a more linear fashion later on. When the PAEKI sample zone was migrated to 95% L_d, the broadening profile was close to that of hydrodynamic injection. The threshold for band broadening in PAEKI sample zones decreased with increasing electromigration distance from the inlet end in the capillary, indicating that different factors influence broadening compared to hydrodynamically injected plugs. This result implies that factors other than simple diffusion influence the width of the analyte zone. The observation of a distinct threshold time indicates that external forces suppress diffusion in PAEKI which is supportive of the concept of a counter-ion layer. Band broadening occurred after the counter-ion layer became destabilized, either by sufficient diffusion time in 0 V cm^{-1} field or physically during electromigration. In the case of PAEKI samples zones migrated to 95% L_d, we propose the that counter-ion layer was disrupted due to the physical separation of

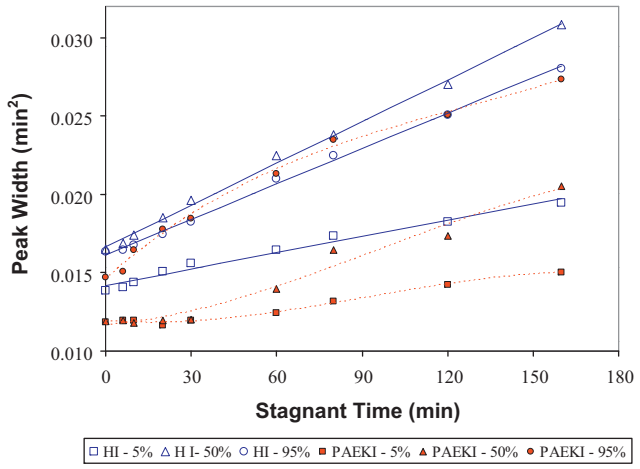

Fig. 2. Diffusion profile of sample zones injected by hydrodynamic pressure and PAEKI. Diffusion was measured by FWHM^2 as a function of both stagnant time and the position in the capillary (denoted as % of L_d) for comparison of PAEKI with hydrodynamic injection (denoted as HI). Data for hydrodynamic pressure profiles were best fit linearly where PAEKI profiles were fit to third order polynomials in order to illustrate differences in diffusion profiles ($R^2 > 0.97$ for all profiles). Conditions: −6 kV, +50 mbar, 3 min, 500 ng mL^{-1} d-AMP sample for PAEKI; +50 mbar, 5 s, 500 μg mL^{-1} d-AMP sample for hydrodynamic injection; 20 mmol L^{-1} of ammonium carbonate, pH 9.2 BGE; 75 cm L_T, 66.5 cm L_d, i.d. 50 μm, 20 °C capillary. After injection, sample zones were migrated to different positions in the capillary by electroosmotic flow (+30 kV for 0.5, 4 or 7.5 min) and allowed to diffuse prior to separation (+30 kV).

the anionic analyte layer from the cation layer by differences in μ_{ep}, as hypothesized in Fig. 1d. In this situation, as no counter-ion layer remains to electrostatically stabilize the anionic sample zone and hinder broadening, the lateral analyte diffusion occurs more readily in 0 V cm^{-1} field, similar to the corresponding hydrodynamic injection. Furthermore, it was observed that peak width for PAEKI at 95% L_d was greater than for both 5 and 50% L_d, likely indicating that the counter-ion layer was disrupted during electromigration after it had travelled between 50 and 95% of the capillary length.

In general, PAEKI resulted in narrower peaks than the corresponding hydrodynamic injection. This observation was not surprising because although the methods were designed so that comparable quantities of analyte were injected, the focusing that occurred during PAEKI resulted in a smaller zone being injected for the same analyte quantity. Noteworthy at 95% L_d, PAEKI and hydrodynamic injection band broadening was statistically similar from a stagnant time of 10–160 min. Sample zones at 95% L_d diffused at similar rates for PAEKI with $y = (7.2 \pm 0.6) \times 10^5 x + (0.0165 \pm 0.0005)$, $R^2 = 0.9713$ and hydrodynamic injection with $y = (7.2 \pm 0.2) \times 10^5 x + (0.0161 \pm 0.0002)$, $R^2 = 0.9967$, regardless of injection type. This indicates that the counter-ion layer was damaged during the electromigration from inlet end to 95% L_d position. Interestingly, the PAEKI initial peak width was narrower than the corresponding hydrodynamic sample plug, which demonstrates the effectiveness of PAEKI for generating narrow sample bands during injection. Presumably, after destabilization of the counter-ion layers by migration, no remaining counter-ion layer existed and analyte diffusion was no longer influenced by electrostatic forces thereby returning the diffusion profile to that of hydrodynamic injection.

3.3. The influence of organic solvent

Organic solvents are well known as additives to both sample and separation buffers to influence the properties of the solution. Organic solvent added to sample solution can enhance pre-concentration as in HC-FASS [40], whereas in the BGE it can

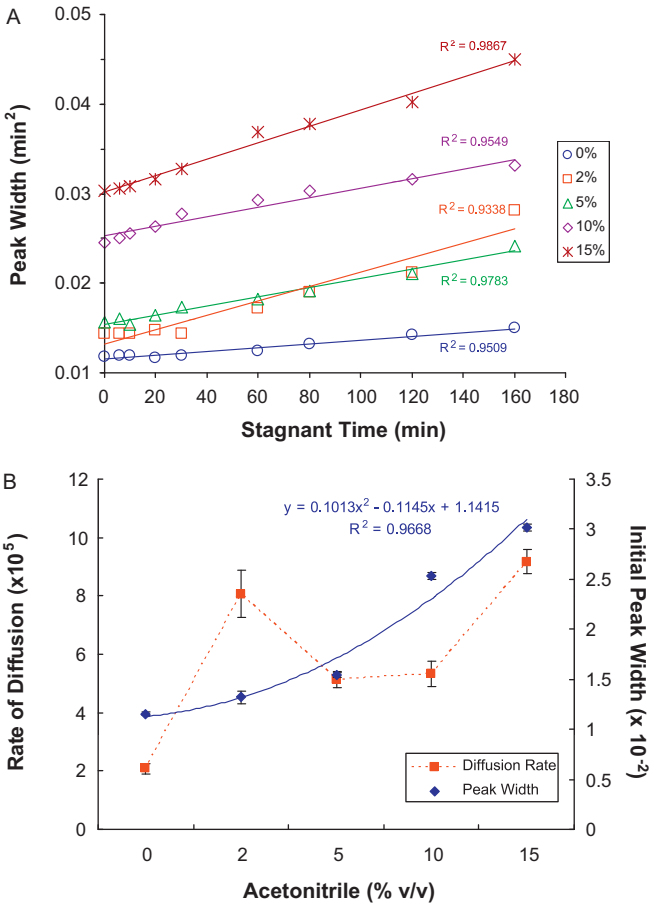

Fig. 3. Influence of acetonitrile in the BGE in PAEKI where (A) shows a linear increase in peak diffusion as seen by an increase in peak width with increasing stagnant time and (B) shows the relationship between rate of diffusion and initial peak width with increasing ACN. Note that despite the increasing peak width, the quantitative relationship with acetonitrile is nonlinear. Data for intercept values are fit to a 2nd order polynomial to illustrate trend whereas no fit was satisfactory for slope data. The units for rate of diffusion are min^2 (FWHM^2) per min where the initial peak width is measured as FWHM^2. Conditions: 20 mmol L^{-1} of ammonium carbonate pH 9.2 with 0, 2, 5, 10 or 15% ACN BGE; +30 kV; PAEKI and CE conditions same as Fig. 1. The sample zone was migrated 5% of the capillary length (+30 kV for 0.5 min) after injection.

suppress the EOF, increase solubility of other additives or analytes, as in MEKC, or decrease the conductivity of the solution [18,41]. Previously, we showed that ACN impacts the concentration of analyte injected by increasing buffer resistivity (lowering γ in Eq. (1)). In our current study, we used ACN to modify the mobility of the analytes by changes in η and ϵ.

Figs. 3 and 4 depict the relationship between diffusion profiles of analyte bands to various concentrations of ACN in the BGE for PAEKI and hydrodynamic injections, respectively. As can be seen in Fig. 3a, there was an increase in peak width with increasing concentrations of ACN which indicates an increase in analyte diffusion mobility. However, this increase was not due solely to diffusion. As can be seen in Fig. 3b, the amount of ACN added to the BGE resulted in a non-linear increase in initial peak width, where tripling the amount of ACN from 5 to 15% caused the initial peak width to double. The relationship between initial peak width and %ACN could be expressed by a polynomial function ($y = 0.1013x^2 - 0.1145x + 1.1415$, $R^2 = 0.9668$); however no clear statistical relationship could be determined between %ACN and diffusion rate, despite an observable increasing trend. When compared to hydrodynamic injection, there was also an observed increase in diffusion seen with increase in ACN

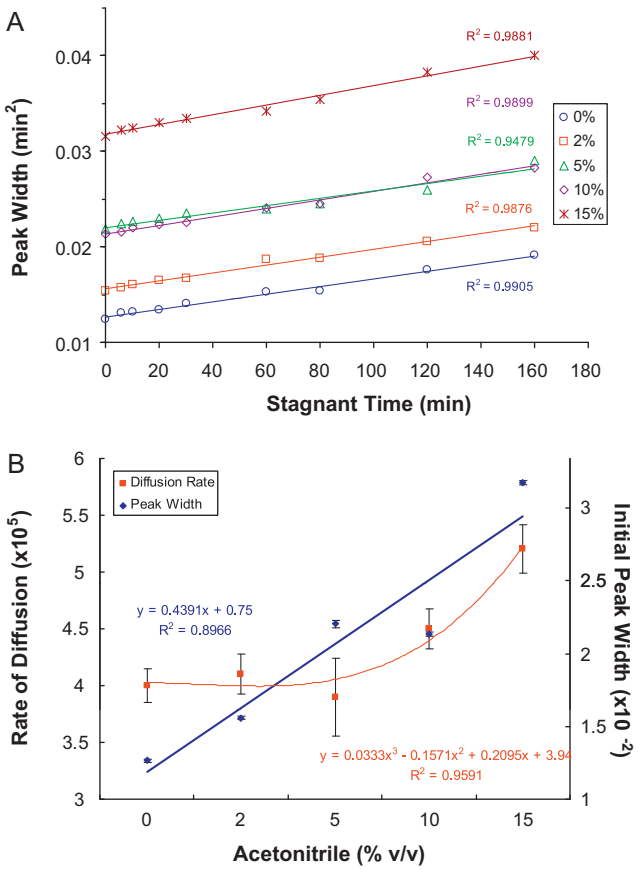

Fig. 4. The influence of the acetonitrile on hydrodynamic injection where (A) shows a linear increase in peak diffusion as seen by an increase in FWHM^2 with increasing stagnant time. The quantitative relationship is given in (B). Intercept data displayed a linear relationship with acetonitrile concentration throughout the range tested whereas slope data was linear only at concentrations greater than 5%. Data for slope values were fit to a 3rd order polynomial to illustrate trend. Conditions: 20 mmol L^{-1} of ammonium carbonate pH 9.2 with 0, 2, 5, 10 or 15% ACN BGE; +30 kV; PAEKI and CE conditions same as Fig. 1. The sample zone was migrated 5% of the capillary length (+30 kV for 0.5 min) after injection.

(Fig. 4a), however, the relationship was linear for initial peak width ($y = 0.4391x + 0.75$, $R^2 = 0.8966$); and clearly non-linear for slope ($y = 0.0333x^3 - 0.1571x^2 + 0.2095x + 3.94$, $R^2 = 0.9591$; Fig. 4b).

The differences in the relationships between initial peak width and ACN were not surprising given the nature of the injection methods employed. Since addition of ACN lowers the viscosity of the BGE and thereby decreases the frictional resistance of analyte migration, it serves to reason that laminar flow profile of the pressure injection likely becomes more parabolic. Subsequently, the surface area of the plug boundary increases, promoting the diffusion of the analyte into the BGE during injection with increasing ACN. In PAEKI, where the plug boundary is presumed to be reasonably flat, due the nature of the EOF, the impact by small increases in ACN (0–5%) on peak width was not obvious. However, with a concentration of ACN greater than 5% in buffer, band broadening perceptibly occurred. This may indicate that the decrease of conductivity in the BGE by increasing ACN could reduce both the stacking efficiency for concentrating analytes into the sample plug (due to the decrease of γ value) and the capacity for formation of the cation counter-ion layer (i.e. the counter-ion layer charge density decreases with increasing ACN). Thereby, the strength of the soft counter-ion boundary was decreased, which consequently reduced the forces suppressing broadening and likely promoted permittivity of stacked analytes through the boundary. This observation was consistent with our previous results that indicated addition of ACN to the BGE was detrimental to loading in PAEKI.

Since the addition of ACN to the BGE is known to influence both η and ϵ, we expected to observe a perturbation to stability of the counter-ion layer formed during PAEKI. We hypothesized that the lifetime of the counter-ion layer would decrease since decreasing η and changing ϵ would increase the rate of lateral diffusion. As can be seen in Fig. 3b, although no satisfactory relationship could be statistically fit to the data, there is general increasing trend in the rate of diffusion with increasing ACN. The scatter in the data may be attributed in the increasing instability of the counter-ion layer, compounded by increasingly inefficient sample loading, which could increase the difficulty in obtaining a clear relationship. When compared to simple hydrodynamic injection (Fig. 4b), it can be seen that the changes to rate of diffusion occur only at concentrations of ACN greater than 2%. This concentration may indicate the threshold concentration for observable changes in lateral diffusion of the sample plug. At concentrations of ACN greater than 2%, there was a linear relationship between increasing rate of diffusion with ACN; $y = (1.30 \pm 0.06) \times 10^{-6}x + (3.23 \pm 0.06) \times 10^{-2}$, $R^2 = 0.998$. This effect can be solely attributed to the decrease in η since there were no electrostatic effects to perturb by changing ϵ. By contrast, in PAEKI, the rate of diffusion can be expressed by $y = (4 \pm 2) \times 10^{-6}x + (2.5 \pm 2.2) \times 10^{-2}$, $R^2 = 0.785$ from 5 to 15% ACN. Despite the larger error, it is obvious that diffusion is not increasing by the same proportion for the two methods (rate = 1.30 ± 0.06 vs. 4 ± 2). This comparison further supports that in PAEKI a counter-ion layer was formed, in which stability was perturbed by altering both η and ϵ.

3.4. The influence of analyte mobility

We previously noted that the electrophoretic mobility of analyte, $\mu_{ep,A}$, affects sample loading in PAEKI [36]. We further showed that peak width is independent of sample loading, i.e. PAEKI injection plugs are similar in size for a given analyte under given PAEKI conditions regardless of initial sample concentration [37]. However, the influence of $\mu_{ep,A}$ on the sample plug size had not yet been studied. Four analytes with very different negative $\mu_{ep,A}$, d-AMP < arsenate [$HAsO_4^{2-}$] < selenite [SeO_3^{2-}] < bromate (BrO_3^-), were chosen to investigate the influence of the ion mobility. To maintain the same amount of analyte injected in each sample plug, the concentrations of samples were diluted in inverse proportion to PAEKI injection time (Table 1). A voltage of +30 kV was applied to separate the analytes after injection. Fig. 5 showed that with increasing negative $\mu_{ep,A}$ the peak width increased. Furthermore as PAEKI time was increased, the peak width increased for all analytes except for d-AMP (Fig. 5a), indicating that only the analyte with the slowest $\mu_{ep,A}$ was efficiently immobilized at the boundary during PAEKI, which was consistent with our previous observation that analytes with low $\mu_{ep,A}$ are more efficiently concentrated in PAEKI. Given the formation of a positive counter-ion layer at the BGE side of the boundary via electrostatic attraction, the observations in Fig. 5 can be explained in terms of the differences in interaction with the counter-ion layer depending on their physicochemical properties.

Analytes with low $\mu_{ep,A}$, form a negative layer at the boundary according to stacking theory, however the larger hydrodynamic radius physically impedes their migration through the positive cation layer thereby increasing the pre-concentration efficiency. Furthermore, as the analyte size decreases (R_H), there is less hydrodynamic drag impeding migration through the positive counter-ion layer. This is supported by calculation of the Connolly Solvent Excluded Volume (ChemBio Office 2010, Chem 3D Pro) where analyte volumes were found to be 44 Å^3 BrO_3^- < 46 Å^3 SeO_3^{2-} < 53 Å^3 $HAsO_4^{2-}$ < 208 Å^3 d-AMP. Clearly, d-AMP, more than 4 times larger

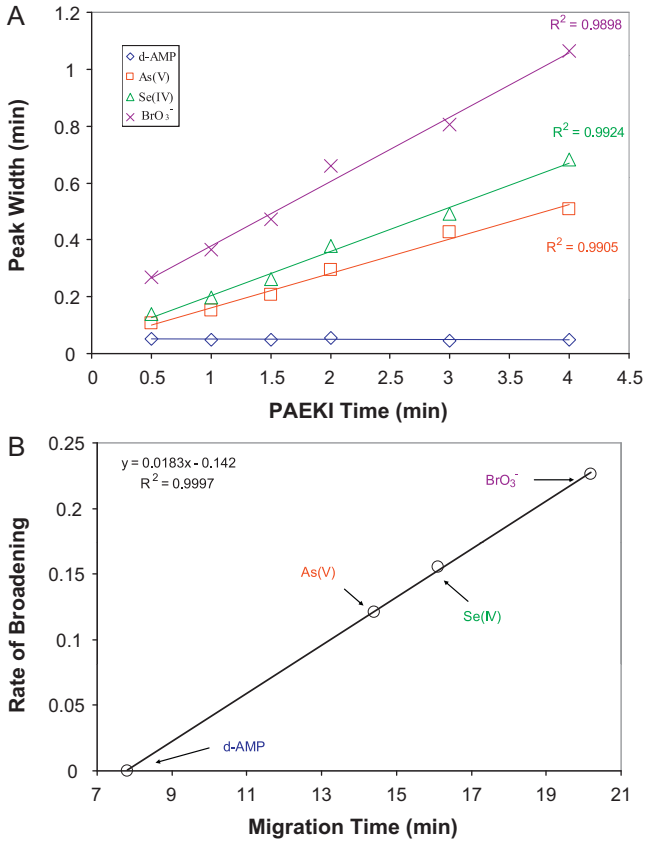

Fig. 5. The effect of analyte electrophoretic mobility on PAEKI where (A) shows the increase in peak width as a function of PAEKI time and (B) shows the relationship between the rate of sample zone broadening and analyte migration time. PAEKI injection conditions and concentrations of analytes in sample solutions are listed in Table 1. All other conditions are the same as in Fig. 1.

than BrO_3^-, would be less subject to forces of diffusion due to its larger size and would experience greater hydrodynamic drag as compared to the smaller BrO_3^- anion. Moreover, given the pK_a's of the analytes studied, the expected charge order is d-AMP (pK_a = 6.85) > $HAsO_4^{2-}$ (pK_a = 7) > SeO_3^{2-} (pK_a = 8.27) > BrO_3^- in a neutral pH sample solution. Therefore analyte charge would also play an important role in PAEKI stacking efficiency, where d-AMP stacks most efficiently due both its greater negative charge and larger size which hinders diffusion across the counter-ion boundary.

Both analyte size and charge influence $\mu_{ep,A}$ and thereby PAEKI behaviour. As $\mu_{ep,A}$ increases, the analyte migrates to the boundary layer with increasing velocity. For negatively charged analytes with small R_H, as charge is increased, the positive charge at the boundary may no longer be a sufficient attractive electrostatic force to hold the analyte stationary. Longer PAEKI times allow more analyte to cross the boundary, hindering formation of a stable counter-ion layer. Peak width ultimately increases, with the rate of broadening increasing as a function of PAEKI time depending on $\mu_{ep,A}$ (Fig. 5b). Here, $\mu_{ep,A}$ is represented in magnitude by migration time with BrO_3^- possessing the largest – $\mu_{ep,A}$ and therefore the longest migration time. It can be seen that there is a linear relationship between the rate of PAEKI broadening and migration time. Therefore, where analytes with low $\mu_{ep,A}$ can be pre-concentrated by PAEKI for theoretically infinite lengths of time, injection time for analytes with high $\mu_{ep,A}$ must be optimized to obtain the highest loading possible without detrimental broadening.

3.5. Detection of inorganic anions in drinking water

PAEKI with CE-ESI-MS/MS was used to analyze drinking water samples for common toxic ions, some of which are the by-products of disinfection. In order to evaluate the analytical performance of PAEKI-CE-ESI-MS/MS for drinking water analysis, standard solutions of arsenite [AsO_2^-], arsenate [$HAsO_4^{2-}$], selenite [SeO_3^{2-}], selenate [SeO_4^{2-}] and bromate [BrO_3^-] were prepared and analyzed. Analytical performance characteristics are given in Table 3. Calibration curves were constructed and found to be linear over a broad range, from 5 to 5000 ng mL^{-1} ($y = 0.05561x - 0.00062$ and $R^2 = 0.9998$ for As(V); $y = 0.4758x + 0.0711$ and $R^2 = 0.9942$ for Se(VI); $y = 0.2008x + 0.0193$ and $R^2 = 0.9995$ for Se(IV); $y = 0.0775x + 0.0015$ and $R^2 = 0.9998$ for As(III) and $y = 0.2905x + 0.036$ and $R^2 = 0.9971$ for bromate) The method detection limit (MDL) in this study was found to range from 1.0 to 3.0 ng mL^{-1}. The repeatability of PAEKI injection was evaluated by repeated injection ($n = 6$) of a 50 ng mL^{-1} standard mixture solution. The relative standard deviation (RSD) ranged from 6.0 to 13.5%. Table 3 also outlines the recoveries of the five analytes spiked into tap water. Recovery experiments were performed with 50 and 500 ng mL^{-1} final concentration spikes. When the water samples were used untreated, recovery was found to be similar at both concentrations for most analytes with RSD $\leq$27%. However, it was noted that As(III) could not be recovered from water samples at 50 ng mL^{-1} spikes. When the spike concentration was increased, As(III) was recovered, but only in residential water samples. This result indicated that there was a difference in the matrix composition of the commercial and residential water samples. It was hypothesized that As(III), which is known to be neutral below pH 9 [9], was unionized in the tap water samples. Since PAEKI can only pre-concentrate charged analytes, it follows that neutral As(III) could not be loaded onto the capillary column by PAEKI. Therefore in order to recover the As(III), water samples were treated with NaOH in order to increase the pH and ionize As(III). Under this treatment condition, As(III) was recovered at both 50 and 500 ng mL^{-1} spike concentrations. The respective total ion electropherograms comparing the two conditions are shown in Fig. 6a and b, respectively. Note the absence of As(III) in Fig. 6a and the appearance of a sharp As(III) peak when the pH of the sample solution is increased by addition of NaOH (Fig. 6b). However, despite the improvement in As(III) detection by sample basification, pK_a alone does not explain the selective recovery of As(III) in office versus residential samples since all water samples were measured to possess similar pH. Furthermore, a standard solution of As(III), prepared in DI water at neutral pH, was detected via PAEKI injection (data not shown). This clearly demonstrates that some anionic As(III) must be present at neutral pH for successful PAEKI. We therefore suspect that the matrix of residential water differs from commercial water in a manner that interferes with As(III) detection. Although we were unable to determine the exact source of interference, we surmise that interference is likely chemical in nature, chelation or chemical species for example, since addition of NaOH was sufficient to disrupt the mechanism of interference and promote recovery As(III).

Interestingly, as shown in Fig. 6a, analysis of the tap water samples without pre-treatment yielded a narrow Se(VI) peak at a migration time about 5 min different than the treated sample (Fig. 6b). The migration times were the same for Se(VI) in the treated sample and hydrodynamically injected standard (data not shown), therefore it could be reasonably assumed that the form of the Se(VI) species in the untreated tap water was different to that in the treated water samples. We suspect that the migration time of Se(VI) in the tap water was shifted by the formation of a non-covalent species such as a selenate–water complex. A non-covalent species would affect $\mu_{ep,A}$ by a change in z and/or R_H, but

Table 3
Analytical performance characteristics for analysis of anionic drinking water contaminants.

Analyte	MDL[a] (ng mL^{-1})	RSD (%)	% Recovery[b]			
			Untreated		Treated	
			50 ng	500 ng	50 ng	500 ng
As(III)	1.8	6.5	–	90 ± 10[c]	97 ± 7	100 ± 13
As(V)	3.0	7.7	102 ± 23	109 ± 14	105 ± 23	94 ± 12
Se(IV)	1.0	14	93 ± 27	109 ± 8	118 ± 26	98 ± 10
Se(VI)	1.4	6.0	107 ± 10	99 ± 13	109 ± 14	103 ± 8
BrO_3^-	1.0	6.8	98 ± 19	91 ± 19	107 ± 15	104 ± 8

[a] MDL: defined as three times the signal/noise.
[b] % Recovery: calculated at spikes of 50 and 500 ng of standard added to 1 mL untreated or treated (5 μL of 0.1 mol L^{-1} sodium hydroxide added per 1 mL sample) water sample; data is an average of triplicate measurements (n = 3) of each water sample sources (N = 4). As(III) was not detected after 50 ng mL^{-1} spike in all samples.
[c] Calculated from residential water samples only. As(III) was not detected after 500 ng mL^{-1} spike in untreated samples collected from the two office buildings.

also be easily disrupted during the ESI process enabling MS detection at the same precursor ion species. Moreover, a small shift in pH by addition of NaOH would affect the ability to form such non-covalent species. Further experiments are necessary to confirm our hypotheses and identify the exact nature of such species, possibly by modeling migration or use of a softer ionization mechanism to preserve non-covalent complexes at the CE-MS interface. However, the potential of being able to identify different complex species represents an exciting application of PAEKI-CE-MS, where the true speciation of the contaminants in water samples can be identified without the bias created by other pre-concentration techniques in CE or other drinking water analysis methods. Compared to without sample basification, the TIC peak heights of the analytes were dramatically decreased with the alkaline treatment as shown in Fig. 6. We suspect that the alkaline treatment increased the ionic strength in the sample solution thereby decreased the PAEKI efficiency due to γ decrease in the Eq. (1). Additionally, the increase of Na+ from the alkaline treatment with NaOH could also cause a decrease of ionization efficiency in the ESI source.

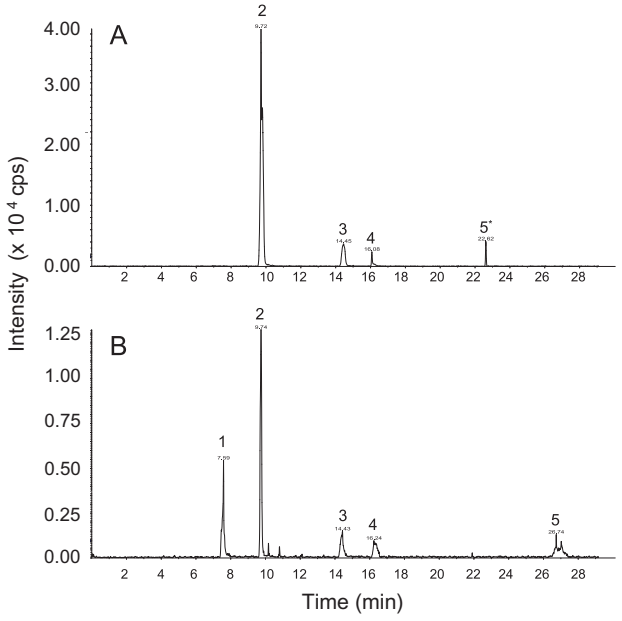

Fig. 6. Representative TIC Electropherograms of analysis of residential tap water spiked with 50 ng mL^{-1} As(III), As(V), Se(IV), Se(VI), and BrO_3-, and 500 ng mL^{-1} d-AMP where water was analyzed by PAEKI without treatment (A) and with treatment of 5 μL of 0.1 mol L^{-1} sodium hydroxide solution (B). CE-ESI-MS conditions: 110 cm L_T, 50 μm i.d. capillary; 20 mmol L^{-1} ammonium carbonate (pH = 9.2) BGE; +30 kV, +50 mbar separation; −7.5 kV, 50 mbar, 3 min PAEKI. Peaks were: 1 = As(III); 2 = d-AMP; 3 = As(V) overlapped with Se(IV); 4 = BrO_3^-; and 5 = Se(VI), and * denotes migration time shift due to matrix effects.

In our analysis of commercial and residential tap water, we found that arsenic, selenium and bromate were undetected in all samples, indicating the target analytes were all lower than the method detection limits. The procedure described in this paper was sensitive enough to measure the targeted analytes as low as 1 ng mL^{-1} which was sensitive enough to detect the analytes at their respective EPA regulated MCLs (10 ng mL^{-1} for arsenic, 50 ng mL^{-1} for selenium and 10 ng mL^{-1} for bromate). Compared to conventional techniques, our method was comparable to ion chromatography, IC-ICP-MS and ICP-MS which have MDLs of 5 ng mL^{-1} for bromate [14], 0.1–0.6 ng mL^{-1} for As [42] and 0.3 ng mL^{-1} for selenium species [43], respectively. However, atomic spectroscopy remained more sensitive for arsenic detection with and MDL of 0.01 ng mL^{-1} for As(III) and 0.009 ng mL^{-1} for total arsenic [44]. Presumably, hyphenation of PAEKI-CE to ICP-MS would increase the method sensitivity for measurement of trace contaminants in drinking water, which may lower the MDL to a level more comparable to atomic spectroscopy. The enhanced method would be additionally advantageous since the molecular species of the target contaminant is maintained in untreated samples.

4. Conclusions

We have proposed a counter-ion layer theory to describe the phenomena observed in PAEKI. The diffusion behaviour of the PAEKI sample plug was studied as a function of analyte diffusion from the sample plug, diffusion resulting from migration as well as the analyte properties during injection. When compared to the diffusion behaviour of hydrodynamically injected plugs and it was found that PAEKI plugs experienced less band broadening overall. The formation of a counter-ion layer at the interface of the plug-BGE boundary was found to counteract diffusive forces since the negative anion sample layer was electrostatically attracted to the cation layer formed at the BGE side of the boundary. Further evidence for formation of the counter-ion layer was the change in PAEKI diffusion profiles, obtained by altering viscosity, conductivity and analyte mobility, properties which all contributed to the stability of the counter-ion layer. Acetonitrile in buffer reduced the enhancement factors of the technique by decreasing viscosity and ionic strength of the BGE and analytes with the higher mobility had a broader sample plug length than those with the lower mobility due to increased ability to cross the soft cation layer. With a better understanding of PAEKI for CE-ESI-MS/MS, we were able to optimize and validate the method for ng mL^{-1} detection of arsenic, selenium and bromate species in residential and commercial water samples, expanding use of PAEKI to detection of small inorganic anions and demonstrating the potential for analysis of drinking water contaminants.

Acknowledgements

HZ and JMAG are grateful to NSERC Canada and Health Canada for financial support in the form of postdoctoral fellowships. This project was financially supported by the Canadian Government under the Canadian Environmental Protection Act.

References

[1] M. Deborde, U. von Gunten, Water Res. 42 (2008) 13.
[2] S.D. Richardson, Anal. Chem. 75 (2003) 2831.
[3] U. von Gunten, Water Res. 37 (2003) 1469.
[4] A. Chatterjee, D. Das, B.K. Mandal, T.R. Chowdhury, G. Samanta, D. Chakraborti, Analyst 120 (1995) 643.
[5] J.L. Valentine, H.K. Kang, G.H. Spivey, Environ. Res. 17 (1978) 347.
[6] A.B. DeAngelo, M.H. George, S.R. Kilburn, T.M. Moore, D.C. Wolf, Toxicol. Pathol. 26 (1998) 587.
[7] Y. Kurokawa, A. Maekawa, M. Takahashi, Y. Hayashi, Environ. Health Perspect. 87 (1990) 309.
[8] U.S. Environmental Protection Agency, National Primary Drinking Water Regulations, 2009, Retrieved from www.epa.gov/safewater/contaminants.
[9] U.S. Environmental Protection Agency, Drinking Water Treatability Database, 2010, Retrieved from http://oaspub.epa.gov/tdb/pages/general/home.do.
[10] U.S. Department of Health and Human Services, Agency for Toxic Substances and Disease Registry, 2010, Retrieved from http://www.atsdr.cdc.gov.
[11] J.S. Petrick, F. Ayala-Fierro, W.R. Cullen, D.E. Carter, H. Vasken Aposhian, Toxicol. Appl. Pharmacol. 163 (2000) 203.
[12] M.S. Alaejos, C.D. Rornero, Chem. Rev. 95 (1995) 227.
[13] G. Yang, S. Wang, R. Zhou, S. Sun, Am. J. Clin. Nutr. 37 (1983) 872.
[14] R. Butler, L. Lytton, A.R. Godley, I.E. Tothill, E. Cartmel, J. Environ. Monitor. 7 (2005) 99.
[15] S.D. Richardson, Anal. Chem. 81 (2009) 4645.
[16] N.W. Frost, M. Jing, M.T. Bowser, Anal. Chem. 82 (2010) 4682.
[17] C.W. Klampfl, Electrophoresis 27 (2006) 3.
[18] P.R. Haddad, P. Doble, M. Macka, J. Chromatogr. A 856 (1999) 145.
[19] A.R. Timerbaev, Electrophoresis 31 (2010) 192.
[20] M.C. Breadmore, Electrophoresis 28 (2007) 254.
[21] S.L. Simpson, J.P. Quirino, S. Terabe, J. Chromatogr. A 1184 (2008) 504.
[22] A. Hori, T. Matsumoto, Y. Nimura, Anal. Chem. 65 (1993) 2882.
[23] M.M. Meighan, J. Vasques, L. Dziubcynski, S. Hews, M.A. Hayes, Anal. Chem. 83 (2011) 368.
[24] R. Klvduee, P. Kuba, K. Vunder, M. Kaljurand, Electrophoresis 21 (2000) 2879.
[25] S. Park, H. Swerdlow, Anal. Chem. 75 (2003) 4467.
[26] Q. Wang, S.-L. Lin, K.F. Warnick, H.D. Tolley, M.L. Lee, J. Chromatogr. A 985 (2003) 455.
[27] Q. Wang, B. Yue, M.L. Lee, J. Chromatogr. A 1025 (2004) 139.
[28] J. Astorga-Wells, H. Swerdlow, Anal. Chem. 75 (2003) 5207.
[29] J. Astorga-Wells, S. Vollmer, T. Bergan, H. Jörnvall, Anal. Chem. 79 (2007) 1057.
[30] J. Astorga-Wells, S. Vollmer, S. Tryggvason, T. Bergan, H. Jornvall, Anal. Chem. 77 (2005) 7131.
[31] S.L. Lin, H.D. Tolley, M.L. Lee, Chromatographia 62 (2005) 277.
[32] J. Quirino, S. Terabe, Anal. Chem. 72 (2000) 1023.
[33] M.C. Breadmore, Electrophoresis 29 (2008) 1082.
[34] M. Dawod, M.C. Breadmore, R.M. Guijt, P.R. Haddad, Electrophoresis 31 (2010) 1184.
[35] Y.-L. Feng, H. Lian, J. Zhu, J. Chromatogr. A 1148 (2007) 244.
[36] Y.-L. Feng, J. Zhu, Anal. Chem. 78 (2006) 6608.
[37] Y.-L. Feng, J. Zhu, Electrophoresis 29 (2008) 1965.
[38] H. Zhang, J. Zhu, Y.-L. Feng, Anal. Sci. 26 (2010) 1157.
[39] J.W. Munch, Method 528: Determination of Phenols in Drinking Water by Solid Phase Extraction and Capillary Column Gas Chromatography/Mass Spectrometry (GC/MS), U.S. Environmental Protection Agency, Cincinati, 2000.
[40] C.X. Zhang, W. Thormann, Anal. Chem. 68 (1996) 2523.
[41] E. Kenndler, M.L. Riekkola, Electrophoresis 28 (2007) 3579.
[42] A.J. Bednar, J.R. Garbarino, M.R. Burkhardt, J.F. Ranville, T.R. Wildeman, Water Res. 38 (2004) 355.
[43] W.J. Christian, C. Hopenhayn, J.A. Centeno, T. Todorov, Environ. Res. 100 (2006) 115.
[44] R. Liu, P. Wu, M. Xi, K. Xu, Y. Lv, Talanta 78 (2009) 885.